

Study of petrolatum structure: Explaining its variable rheological behavior

A.J.P. van Heugten^{a,b,*,1}, J. Landman^{c,d,1}, A.V. Petukhov^{c,e}, H. Vromans^{a,b,f}

^a Department of Pharmaceutics, Utrecht Institute for Pharmaceutical Sciences, Utrecht University, 3584 CG Utrecht, The Netherlands

^b Research and Development Department, Tiofarma B.V., Hermanus Boerhaavestraat 1, 3261 ME Oud-Beijerland, The Netherlands

^c Van't Hoff Laboratory for Physical and Colloid Chemistry, Debye Institute for Nanomaterials Science, Utrecht University, Padualaan 8, 3584 CH Utrecht, The Netherlands

^d European Synchrotron Radiation Facility, 71 Avenue des Martyrs, 38000 Grenoble, France

^e Laboratory of Physical Chemistry, Eindhoven University of Technology, 5600 MB Eindhoven, The Netherlands

^f Department of Clinical Pharmacy, Division of Laboratory Medicine & Pharmacy, University Medical Centre Utrecht, P/O Box 85500, 3508 GA Utrecht, The Netherlands



ARTICLE INFO

Keywords:

Petrolatum

Rheology

Synchrotron X-ray

Nanostructure

Microstructure

ABSTRACT

The rheological properties of petrolatum are dependent on both temperature and thermal history. How this thermal dependency can be explained is unclear. In the past it has been suggested that the structure of petrolatum consists of a three-dimensional crystalline network. This has been established using old microscopic techniques only. Therefore a study on the microstructure of petrolatum was conducted using rheometry, DSC, pulsed NMR, polarized light microscopy and synchrotron X-ray. The combination of these techniques show that petrolatum is composed of 21% solid material at room temperature. This consists of partly crystalline lamellar sheets which are packed in stacks. The occurrence of these lamellar sheets is temperature dependent and the number of lamellar stacks is dependent on thermal history. It was shown that rheological differences in petrolatum can be explained by the number of lamellar stacks present, where more lamellar stacks result in more rigid petrolatum.

1. Introduction

Petrolatum is one of the most commonly used materials in pharmaceutical and cosmetic ointments and creams. In 2014 approximately 80 million kg of petrolatum was used for pharmaceutical purposes worldwide (*Microcrystalline Wax and Petrolatum: Global Market Analysis and Opportunities*, 2018). Therefore it can be considered a major bulk product for pharmaceutical applications. For petrolatum and other semi solids physical characterization methods are used to describe its consistency. Since it is a viscoelastic material, meaning it combines both viscous and elastic characteristics, its rheological properties are complex. It behaves non-Newtonian and its structural properties are greatly dependent on temperature and applied shear. The rheological properties can be studied in more detail using oscillatory stress testing (Pandey and Ewing, 2008; Park and Song, 2010; van Heugten et al., 2017a,b). Significant differences in rheological properties exist both between petrolatum grades and different thermal treatments (van Heugten et al., 2017a,b).

Understanding what causes differences in rheological properties is essential to optimise manufacturing processes and formulations (Eccleston et al., 2000; van Heugten et al., 2017a,b). For creams a wide

range of studies is described explaining their rheological properties using techniques such as small angle and wide angle X-ray diffraction (SAXS and WAXS, respectively), differential scanning calorimetry (DSC), thermal gravimetric analysis (TGA) and both electronic and light microscopy (de Vringer et al., 1984; Eccleston, 1986; Junginger, 1984, 1997; de Vringer et al., 1987a,b). Since creams contain water, the focus in characterizing these products generally lies on the location of water within the formulation to define whether it is free or bound to structures within the cream. Others focus on the emulsifiers or other distinctive components within the cream. However this does not apply to petrolatum, since it contains no water or emulsifiers but merely consists of alkanes of varying size (Barry and Grace, 1971). Therefore it is more difficult to determine how differences in rheological properties for petrolatum can be explained.

In literature the explanation of differences in rheological properties for semi-solids is often attributed to the gel network paradigm (Eccleston et al., 2000). Such a gel network forms a viscoelastic continuous phase in emulsions. For petrolatum the structure is generally described as a two-phase system consisting of a three-dimensional crystalline network consisting of fibre-like crystals that encloses and immobilizes the liquid hydrocarbons (Barry and Grace, 1971; Pajor

* Corresponding author at: Department of Pharmaceutics, Utrecht Institute for Pharmaceutical Sciences, Utrecht University, 3584 CG Utrecht, The Netherlands.

E-mail address: tvheugten@tiofarma.nl (A.J.P. van Heugten).

¹ Both authors contributed equally.

et al., 1967; Pandey and Ewing, 2008; Park and Song, 2010; Pena et al., 1994). No clear evidence exists of this three-dimensional crystalline structure. All cited papers conclude that such a structure may explain the complex rheological behaviour of petrolatum but direct evidence has not yet been described.

Nowadays new techniques exist to determine structures within materials such as petrolatum. Especially synchrotron X-ray scattering techniques can be powerful in studying structures at detailed level (Narayanan et al., 2017). This may finally elucidate the microstructure of petrolatum responsible for its greatly variable rheological properties.

Therefore we aim to study the nano-, micro- and macrostructure of petrolatum by synchrotron SAXS and WAXS methodologies combined with DSC, pulsed nuclear magnetic resonance (NMR), hot stage polarised light microscopy (HSPLM) and rheometry.

2. Materials and methods

2.1. Materials

Petrolatum (Snowwhite N, Sonneborn, Amsterdam, The Netherlands) and paraffin oil (Gustav Heess, Leonberg, Germany) were used.

2.2. Rheometry

A stress-controlled rheometer (TA instruments HR-2, Etten-Leur, The Netherlands) equipped with a peltier plate and a 40 mm sand-blasted parallel plate (TA-instruments plate geometry 40 mm) was used. Approximately 5 g of petrolatum was placed on the peltier plate before slowly lowering the upper plate to the preset trimming gap of 1050 μm . After trimming excessive petrolatum the geometry gap was set to 1000 μm .

The linear viscoelastic region (LVR), meaning the range of stresses within which the structure of the sample is not destroyed (Pandey and Ewing, 2008), was determined using oscillatory stress sweep (OSS) experiments in a wide stress range (1–2000 Pa) at 25, 35, 45 and 55 °C. Temperature ramps were conducted within the LVR of 55 °C at a heating and cooling rate of 5 °C/min between 25 and 75 °C. Petrolatum yield stress after slow and fast cooling was determined using a conditioning temperature ramp of 0.1 or 10 °C/min and a OSS similar to the LVR measurements after this temperature ramp. Yield stress was defined as the point where the storage and loss modulus lines cross. Data was analyzed using Trios v3.3.0.4055 software.

2.3. Differential scanning calorimetry (DSC)

DSC measurements were conducted on a TA Instruments Discovery DSC (TA Instruments, Etten-Leur, The Netherlands). 5–8 mg of petrolatum was placed in DSC hermetic aluminum pans and the sample was conditioned at 10 °C for 10 min, next, the sample was heated at 5 °C/min to 70 °C and subsequently cooled to 10 °C at 5 °C/min. Data was analyzed using Trios v3.3.0.4055 software.

2.4. Solid fat content (SFC)

Petrolatum was transferred to a glass NMR tube and stored at room temperature for two weeks. Before measurement the sample was conditioned in waterbaths (Lauda Ecoline RE104, New Jersey, USA) at 10, 15, 20, 25, 30, 35 and 40 °C for 30 min. Afterwards, pulsed NMR (Bruker Minispec MQ20, Leiderdorp, The Netherlands) was used according to the direct method (Coupland, 2001).

2.5. Hot stage polarised light microscopy (HSPLM)

A small amount of sample was applied to a glass slide. All samples were analyzed at a 100 \times magnification on a Nikon Eclipse TE2000-U

microscope (Nikon Instruments Europe BV, Amsterdam, The Netherlands). The samples were assessed at different temperatures. The sample was heated to 25 °C, then 35 °C and 50 °C and finally cooled back to 25 °C. The estimated average heating rate was 4 °C/min, the estimated average cooling rate was 2 °C/min. Pictures were analyzed using ImageFocus v 3.0.0.2.

2.6. Synchrotron small- and wide-angle X-ray scattering

For small- and wide-angle X-ray scattering (SAXS and WAXS) measurements, a small amount of sample was transferred to 80 mm glass capillaries with a diameter of 1 mm and wall thickness of 0.01 mm (Hilgenberg GmbH, Malsfeld, Germany). The sample was heated homogeneously in an oven to 75 °C to remove stresses caused by sample loading. One sample was melted and cooled directly by removing it from the oven at an estimated cooling rate of 10 °C/min. Another sample was allowed to cool to room temperature at a programmed cooling rate of 0.1 °C/min in an oven. Both samples were incubated at room temperature for at least 2 weeks prior to the measurements. After collecting the SAXS/WAXS data for the two samples at room temperature, the fast cooled sample was subject to a thermal treatment protocol as in the rheological measurements.

SAXS and WAXS patterns were obtained at the DUBBLE beamline at the European Synchrotron Radiation Facility in Grenoble (Borsboom et al., 1998). The SAXS sample-to-detector distance was kept at 1.5 m and X-rays with a wavelength of 0.1 nm were used to measure the scattering. A Pilatus 1 M detector was used to record small-angle (λ) scattering profiles. WAXS profiles were recorded using a Pilatus 300 K detector. Background corrections were applied on all azimuthally (integrated across all angles) integrated profiles. Background correction was obtained from scattering recorded from capillaries filled with paraffin oil.

In the SAXS profiles the scattering wavevector q is plotted against the corresponding intensity (I). This scattering wavevector can be viewed as the resolution with which the sample is observed and is calculated using Eq. (1), in which λ is the wavelength of the X-rays and θ the angle of the X-rays.

$$q = \frac{4\pi}{\lambda} \sin \frac{\theta}{2} \quad (1)$$

2.7. Data analysis

2.7.1. Kratky plot

Before peak analysis, SAXS profiles were multiplied by q^2 to compensate for the inverse square decay (Kratky plot). Such a Kratky plot extracts the slope from the data thereby making the interpretation of the data more reliable since the determination of a peak maximum is more accurate (Glatter and Kratky, 1982).

2.7.2. Porod invariant and peak width σ

Of these Kratky plots the first peaks were integrated as a measure for the amount of material structured in lamellar sheets. This peak integrant corresponds to the so called Porod invariant (Q) (Glatter and Kratky, 1982). A Gaussian curve was fit to each peak and the peak width σ was taken directly from this fitted Gaussian. This peak width is a measure for the degree of periodic order. This corresponds to the number of lamellar sheets in a stack (Glatter and Kratky, 1982). A high peak width reflects a small degree of periodic order and thus a low number of lamellar sheets in a stack.

2.7.3. Crystal lattice, crystallinity and crystallite size

WAXS peak positions were obtained from the azimuthally integrated WAXS profiles from the peak maxima. From these peak positions the type of crystal lattice was determined. For the amount of crystalline material in the sample, the WAXS profiles were multiplied

by q^2 to obtain a Kratky plot. A Gaussian curve was fit to the first peak and a Gaussian was fit to the surrounding background. The ratio of the areas of the Gaussian fit to the first peak and the Gaussian fit to the surrounding background scattering is a measure for the amount of crystalline material in the sample. From the full width at half maximum of the Gaussian fit to the peak we could estimate the size of the crystallites using the Debye-Scherrer equation (Eq. (2)) (Patterson, 1939). In this equation τ represents the mean size of the crystalline domains, K a dimensionless shape factor with a typical value of 0.9, λ the wavelength of the X-ray, β the line broadening at half the maximum intensity and θ the angle (in degrees).

$$\tau = \frac{K\lambda}{\beta \cos \theta} \quad (2)$$

3. Results and discussion

3.1. Macrostructure

3.1.1. Rheometry

A temperature ramp method was conducted on a single petrolatum grade since it is known that thermal history influences the rheological properties of petrolatum (van Heugten et al., 2017a,b). In order to define the influence of the nano- and microstructure of petrolatum on rheological properties this was conducted on a single petrolatum grade as a representative model system. Results are shown in Fig. 1A.

$$|G^*| = G' + iG'' \quad (3)$$

In Fig. 1A on the y-axis a measure for structure of petrolatum is shown, namely the complex modulus $|G^*|$. The $|G^*|$ is the complex sum of the storage modulus (G') and the loss modulus (G'') (Eq. (3)). These two reflect the amount of energy stored in a samples structural interactions when moved, both elastic and viscous. The $|G^*|$ can therefore be considered as the total amount of energy involved in the interactions within a sample. A high $|G^*|$ means a more rigid structure (Pénzes et al., 2004). The $|G^*|$ during cooling is lower than the $|G^*|$ during heating at temperatures above 45 °C. From approximately 50 °C the cooling $|G^*|$ shows a steep increase, becoming higher than the $|G^*|$ of the heating curve from approximately 45 °C. Therefore it can be concluded that petrolatum exhibits a different structure during cooling and heating. The sample becomes more rigid upon cooling than it was before heating. This means that thermal history greatly influences petrolatum structure.

3.1.2. Differential scanning calorimetry (DSC)

The macrostructure of petrolatum can further be evaluated using DSC in which structural characteristics such as melting can be determined (Pettersson et al., 2008a). Results are shown in Fig. 1B.

Fig. 1B shows that during heating endothermic reactions occur

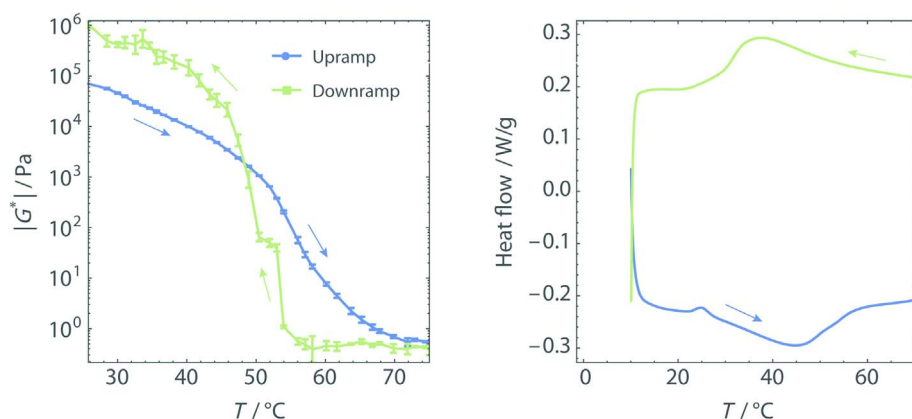


Fig. 1. Viscoelastic properties of petrolatum as a function of temperature. The blue line represents the heating curve and the green line the cooling curve. Measurements were conducted in duplicate at heating/cooling rates of 5 °C/min, SD is shown in error bars (A). Heat flow of petrolatum as a function of temperature at a rate of 5 °C/min. Heating curve is shown in blue and cooling curve is shown in green (B).

Table 1

Solid fat content of petrolatum determined by pulsed NMR.

Temperature in °C	Solid fat content (in % of total mass)
10	24.4
15	23.0
20	21.9
25	20.9
30	19.2
35	16.7
40	14.1

while during cooling exothermic reactions occur. The shape of the peaks during heating and cooling appear slightly different. The enthalpies ($\pm 95\%$ CI) can be calculated by integrating the peaks in the thermogram. During heating the enthalpy is 18.9 (± 1.26) J/g and during cooling 23.1 (± 1.04) J/g. During cooling significantly ($p < 0.05$) more energy is released in forming petrolatum structure than is needed to melt its structure. This is in line with the rheometry data suggesting that during cooling a different structure is formed than the structure that melts during heating (Fig. 1A).

3.1.3. Solid fat content

The solid fat content was determined for petrolatum using pulsed NMR (Table 1). With this method, the amount of solid material can be determined in a sample. The molecules in a solid have different resonance properties than those in liquids. Using NMR these two can be distinguished to quantify their relative proportions (Coupland, 2001).

In Table 1 it can be seen that at lower temperatures petrolatum contains relatively more solid material. At 25 °C this amount is 20.9%. Such a percentage is in line with literature on the composition of petrolatum in general, stating that it consists of only 7–13% high molecular weight paraffins, 30–45% smaller paraffins and 48–60% small paraffins (Barry and Grace, 1971; Gstirner and Meisenberg, 1970). When we assume that the length of the molecules determines whether it is solid or liquid at a certain temperature, it seems logical that all high molecular weight and part of the smaller paraffins are solid at 25 °C.

3.2. Microstructure

3.2.1. Synchrotron small angle X-ray diffraction (SAXS)

To see how the microstructure may influence the rheological properties the structure was studied using synchrotron SAXS measurements. A capillary was filled with petrolatum and exposed to the same temperature protocol as the rheometry measurements of Fig. 1A. In Fig. 2 the results of the SAXS measurements are shown, intensity (I) times q^2 is plotted against the scattering wavevector (q in nm, Eq. (1)).

Fig. 2A and B show several scattering profiles for different measurement temperatures. In some of these, especially at lower

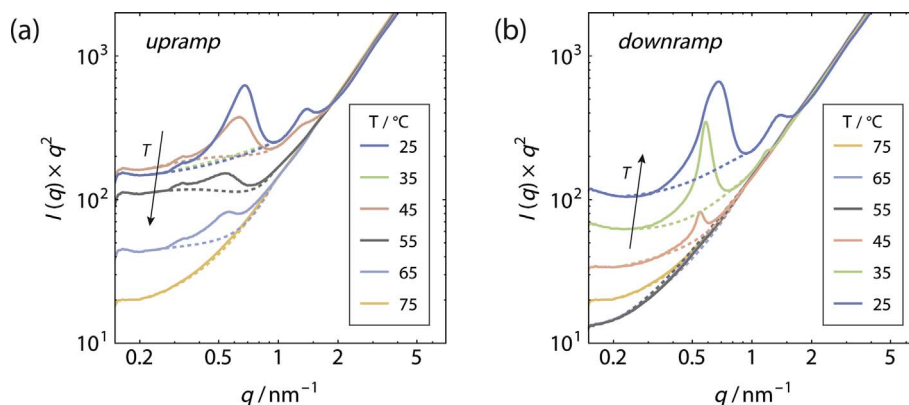


Fig. 2. Kratky representations of the heating (A) and cooling (B) synchrotron small angle X-ray diffraction (SAXS) data. Peak integration lines are shown (dashed).

temperatures, peaks can be observed. These occur around 0.6 nm^{-1} and repeat at around 1.2 nm^{-1} . The peaks start to disappear during heating and are absent above 65°C . When the sample is cooled (Fig. 2B) the peaks start to reappear at temperatures lower than 55°C and show a different, sharper shape than during heating, meaning that SAXS patterns are different during heating and cooling for petrolatum.

The peak pattern in the SAXS measurements indicates the presence of structures in the sample. Based on the fact that the peaks repeat it appears that the peaks are periodic. For SAXS measurements it is known that this is a signature of stacks of lamellar sheets with periodicity in one direction (Chaikin and Lubensky, 1995). The data follows a horizontal trend at small angles. If the structures that are present were smaller than $\sim 1 \mu\text{m}$, the scattering intensity would not have been horizontal within the q -range probed in the experiment. Therefore it seems likely that the length of the lamellar sheets in petrolatum is at least in the micrometer range.

In Fig. 3A the Porod invariant, obtained from the Kratky-representation, was plotted against the temperature. The peak width σ is plotted against temperature in Fig. 3B.

Fig. 3A shows that for the cooled sample the Porod invariant is lower compared to the heating curve except for the data point at 25°C . This means that at 25°C more material is structured in lamellar sheets after cooling than before heating. During cooling however less material is structured in lamellar sheets than during heating at temperatures higher than 25°C . In Fig. 3B the peak width, which corresponds to the number of lamellar sheets in a stack (Glatter and Kratky, 1982), is plotted against temperature. What can be clearly seen is that during heating the peak width increases whilst during cooling the peak width is smaller. The structure of petrolatum can be interpreted as having better defined lamellar stacks during cooling than during heating. At room temperature the standard deviations are similar for both the

starting material and cooled sample (Fig. 3B).

In summary it can now be said that in petrolatum lamellar sheets exist which are ordered in stacks. Their presence and degree of ordering in stacks is temperature dependent.

3.2.2. Influence of cooling rate on petrolatum structure

From the results discussed in the previous sections we can conclude that the lamellar structure of petrolatum is different directly after cooling compared to the starting material. To study whether this difference persists after storage at room temperature, two samples with different thermal history were created (analogues to van Heugten et al. (2017a,b)). One was cooled fast ($10^\circ\text{C}/\text{min}$) and one slow ($0.1^\circ\text{C}/\text{min}$) to room temperature and stored for two weeks. Following this storage period, synchrotron SAXS profiles were obtained at 25°C , as described above.

For these measurements Kratky presentations were made to estimate the Porod invariant and the peak width. All these are shown in Fig. 4.

In Fig. 4A it can be seen that for the slowly cooled sample ($0.1^\circ\text{C}/\text{min}$) sharper peaks are shown. The peak pattern is similar to the pattern shown for the heating and cooling ramp of Fig. 2. Thus the lamellar sheets that arise during the cooling of petrolatum are still present after storage at room temperature for two weeks. Interestingly, no clear difference in Porod invariant for the two thermal treatments exists. Thus similar amounts of material are structured in lamellar sheets for the two samples. The peak width (Fig. 4C) on the contrary, shows a clear difference. The faster cooled sample consists of lamellar sheets that are less ordered or contain less layers than those in the slowly cooled sample. As has been described before petrolatum exhibits a more rigid structure after fast cooling compared to slow cooling (van Heugten et al., 2017a,b). To illustrate this the yield stress, which is a measure for

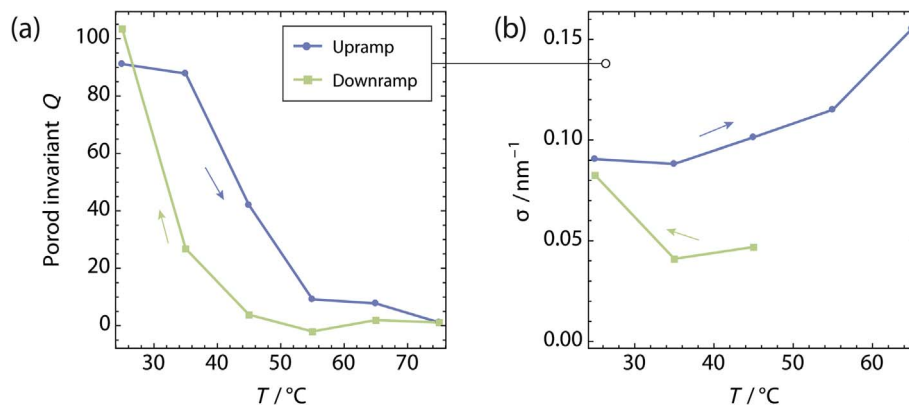


Fig. 3. Porod invariant (Q) integrated from Fig. 3 plotted against the temperature (A). The peak width calculated by fitting a Gaussian curve, expressed as σ/nm^{-1} plotted against temperature for the Kratky plots (Fig. 3) (B).

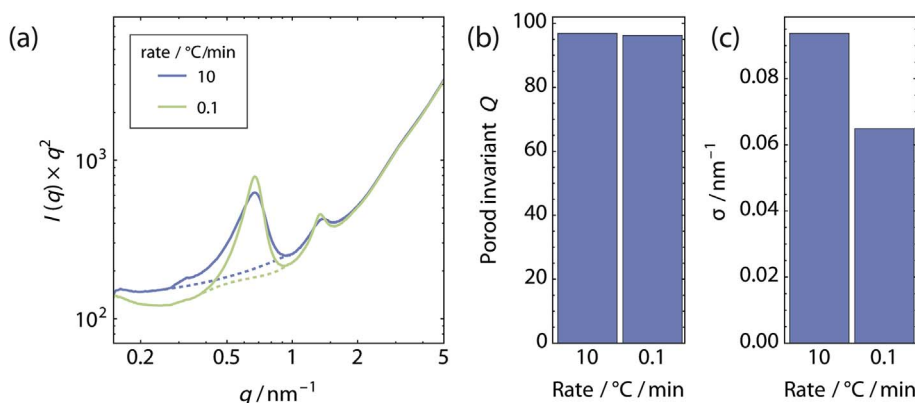


Fig. 4. Synchrotron small angle X-ray diffraction (SAXS) measurements of petrolatum stored for two weeks at room temperature after different thermal treatments in which samples were cooled to room temperatures at different rates, 0.1 and 10 °C/min. (A) represents the Kratky representation of the synchrotron measurements. The area under the first peak of (A) is plotted in (B) as Porod invariant Q and the peak width represented as σ/nm^{-1} by fitting a Gaussian curve to the peak in (C).

the rigidity of petrolatum structure, was measured. For a fast cooled (10 °C/min) sample the yield stress is 1721 Pa and for a slowly cooled (0.1 °C/min) sample 466 Pa. This indicates that not only the number of lamellar sheets but also the degree of ordering of the lamellar stacks influences petrolatum rheology.

3.2.3. Hot stage polarised light microscopy (HSPLM)

To visualise the lamellar stacks in petrolatum HSPLM was performed. Results are shown in Fig. 5.

What can be seen in Fig. 5 is that needle like structures are present in petrolatum of approximately 5–30 μm in size. The amount of these structures is dependent on temperature showing that at 50 °C almost all is melted. Using polarised light microscopy materials can be visualised because of birefringence, meaning a refractive index depending on the polarization of light. Lamellar stacks have a different density compared to the amorphous surroundings and can therefore be visualised using HSPLM. As a result, the observed needle like structures most likely correspond to the lamellar stacks detected in the SAXS measurements. Similar microscopic techniques have previously been used for petrolatum, the observed structures were linked to a three-dimensional crystalline network that encloses and immobilizes the liquid

hydrocarbons (Barry and Grace, 1971; Petersson et al., 2008b; Yamamoto et al., 2014). This however is impossible to conclude on the basis of merely microscopic techniques. Furthermore the suggestion of crystallinity can be better estimated using X-ray diffraction techniques.

3.3. Nanostructure

3.3.1. Synchrotron wide angle X-ray scattering (WAXS)

Using synchrotron WAXS the crystallinity of petrolatum can be determined. Experiments were conducted on the same samples and conditions as the SAXS measurements and results are shown in Fig. 6.

In Fig. 6A several sharp peaks can be seen for both samples, the peaks show similar sharpness and positions for both samples. The sample shows lower peaks after cooling compared to the sample starting material. The peak area is a measure for the amount of crystalline material present. Lower peaks after cooling consequently suggest that the appearance of crystalline order on the nanoscale is lower compared to the starting material. For the samples with different thermal treatments the same peaks can be seen, no clear difference exists between the slowly and fast cooled sample. Therefore it can be concluded that crystal formation is slow and continuous during storage.

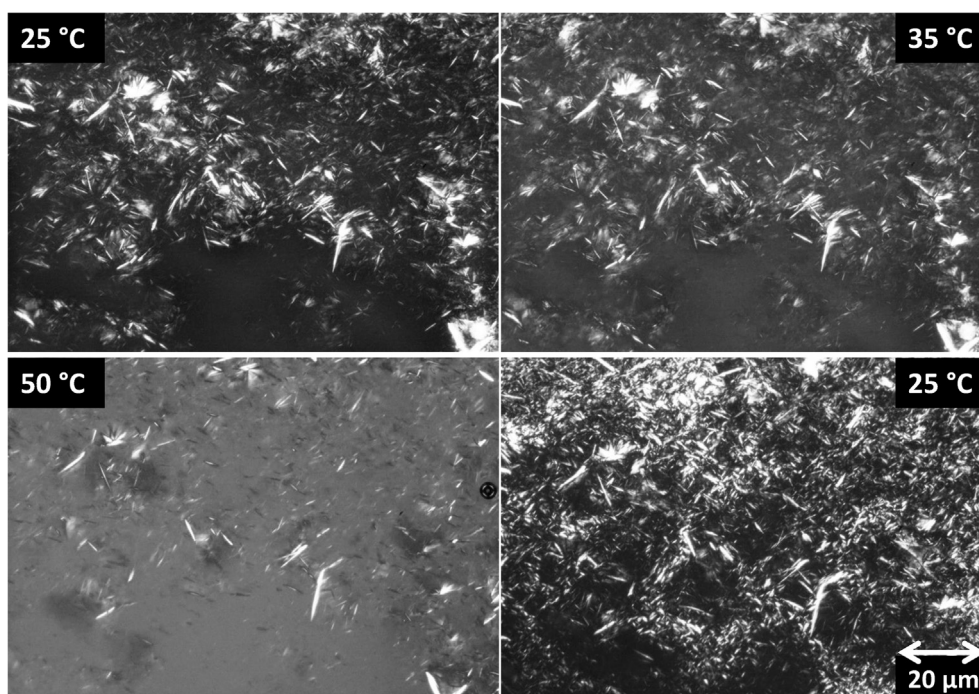


Fig. 5. Hot stage polarised light microscopy (HSPLM) pictures of petrolatum at different temperatures. Magnification was 100 \times , estimated heating rate was 4 °C/min and cooling rate 2 °C/min. Order of the pictures is from left to right.

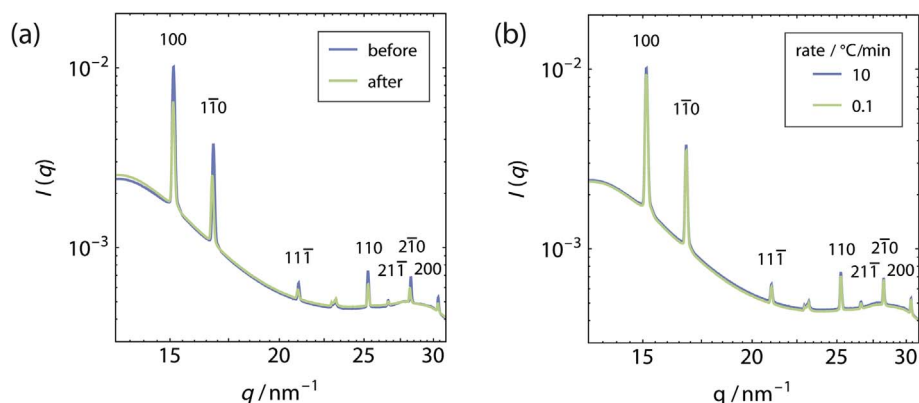


Fig. 6. Synchrotron wide angle X-ray scattering (WAXS) experiments on petrolatum before and after heating and cooling (A) and petrolatum stored for two weeks at room temperature after different thermal treatments in which samples were cooled to room temperatures at different rates, 0.1 and 10 °C/min (B).

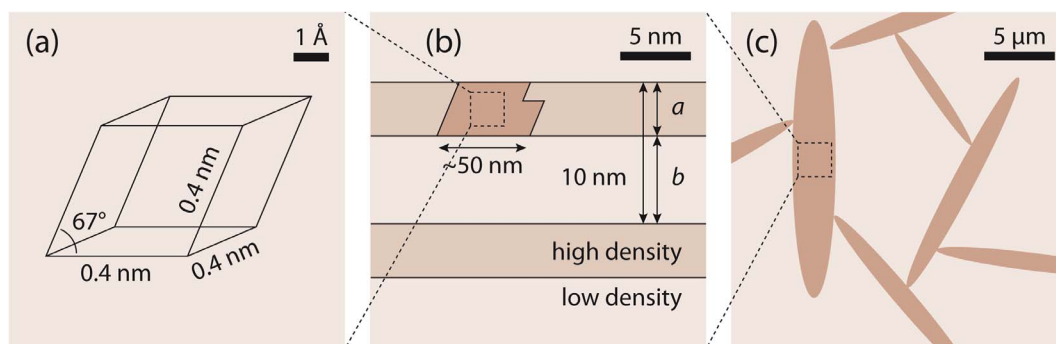


Fig. 7. Schematic overview of the findings on the structure of petrolatum. The Ångstrom scale rhombohedral lattice structure of the crystalline fraction in petrolatum (A), the lamellar structure on a nanoscale (B) and the structure on micrometer scale of interacting lamellar stacks (C) is shown.

The peak positions give information on the crystal lattice and an interpretation of the crystal type is shown in Fig. 7A. The peaks span a rhombohedral lattice with an angle of 113° and a lattice parameter of around 0.4 nm. The larger peaks can all be ascribed to this lattice.

Application of the Debye-Scherrer equation (Eq. (2)) to the width of the first WAXS peak leads to an approximate crystal domain size of up to 50 nm, comparable to what was found in a previous study (van Heugten et al., 2017a,b). The mass fraction of crystalline material was found to be in the order of ~8%. Using pulsed NMR it was shown that at 25 °C 20.9% of petrolatum is solid. If we assume that all solid material in petrolatum is composed of lamellar sheets, ~40% of the lamellar sheets consists of crystalline domains. The percentage of ~8% crystalline material is higher compared to the previously reported value of 1.5% (van Heugten et al., 2017a,b). This difference may be caused by differences in integration method of the WAXS data and/or due to the lower accuracy of the powder X-ray diffractometer used in (van Heugten et al., 2017a,b) compared to the synchrotron WAXS used in the current study.

3.3.2. Synchrotron small angle X-ray scattering (SAXS)

Using synchrotron SAXS not only the length of the lamellar sheets can be estimated but also the thickness of the lamellar sheets can be determined using Eq. (4).

$$d = \frac{2\pi}{q} \quad (4)$$

The periodicity of the lamellar sheets is approximately 10 nm, meaning that lamellar sheets repeat every 10 nm and are most likely separated by lower density liquid. The individual thicknesses of the sheets (a) and lower density fluid (b) are uncertain, however the sum of the two does not exceed 10 nm, as is represented in the Fig. 7B.

3.4. Concluding remarks on petrolatum structure

Fig. 7 represents a graphical summary of our findings on petrolatum nano-, micro and macrostructure. Clearly, on the smallest scale, a fraction of molecules in petrolatum is ordered in a rhombohedral crystal lattice (Fig. 7A), forming crystalline domains of approximately 50 nm (Fig. 7B). The crystalline domains are part of lamellar sheets that repeat every 10 nm in one direction. The formation of the crystals is slow during cooling compared to the lamellar sheets, which form relatively fast. Thermal history primarily influences the degree of ordering of the lamellar sheets in stacks (Fig. 7C). These lamellar stacks make up the macrostructure of petrolatum. The evident influence of the lamellar stacks on the macrostructure of petrolatum is shown in the significant alterations in rheological properties depending on the number of lamellar sheets and lamellar stacks present. The amount of crystalline domains in petrolatum on the other hand does not seem to influence its rheological properties.

Petrolatum is a viscoelastic material and it is now shown that the presence of lamellar stacks can be linked to petrolatum rheological properties. As such, light can finally be shed on the microstructure paradigm. Previously, a fibre-like crystalline network was used to explain the rheological properties of petrolatum (Barry and Grace, 1971; Pajor et al., 1967; Pandey and Ewing, 2008; Park and Song, 2010; Pena et al., 1994). In this study we provide compelling evidence that the fibre-like structures are actually partly crystalline stacks of lamellar sheets that trap the liquid fraction of petrolatum. Therefore a shift in paradigm from a fibre-like crystalline network to a network of partly crystalline lamellar stacks that interact when moved is proposed.

Acknowledgements

We thank Samia Ouhajji, Carla Fernández-Rico and Daniel Hermida-

Merino for their help during synchrotron measurements. The Netherlands Organisation of Scientific Research (NWO) is acknowledged for the allocation of beamtime at DUBBLE at ESRF – the European Synchrotron. This work was supported by the R&D tax credit of the Ministry of Economic Affairs, The Netherlands (grant S016053527). JL acknowledges financial support from NWO (grant 022.004.016) and the ESRF.

References

- Barry, B., Grace, A., 1971. Structural, Rheological and Textural Properties of Soft Paraffins. *J. Texture Stud.* 2.
- Borsboom, M., Bras, W., Cerjak, I., Detollenaere, D., Glastra van Loon, D., Goedtkindt, P., Konijnenburg, M., Lassing, P., Levine, Y.K., Munneke, B., Oversluizen, M., van Tol, R., Vlieg, E., 1998. The Dutch-Belgian beamline at the ESRF. *J. Synchrotron Radiat.* 5, 518–520. <http://dx.doi.org/10.1107/S0909049597013484>.
- Chaikin, P.M., Lubensky, T.C., 1995. *Principles of Condensed Matter Physics*. Cambridge University Press.
- Coupland, J., 2001. Determination of solid fat content by nuclear magnetic resonance. In: *Current Protocols in Food Analytical Chemistry*. John Wiley & Sons, Inc., Hoboken, NJ, USA. <http://dx.doi.org/10.1002/0471142913.fad0301s00>.
- de Vringer, T., Joosten, J.G.H., Junginger, H., 1984. Characterization of the gel structure in a nonionic ointment by small angle X-ray diffraction. *Colloid Polym. Sci.* 262, 56–60. <http://dx.doi.org/10.1007/BF01422578>.
- de Vringer, T., Joosten, J.G.H., Junginger, H.E., 1987a. A study of the gel structure in a nonionic O/W cream by X-ray diffraction and microscopic methods. *Colloid Polym. Sci.* 265, 167–179.
- De Vringer, T., Joosten, J.G.H., Junginger, H.E., 1987b. A study of the ageing of the gel structure in a nonionic O/W cream by X-ray diffraction, differential scanning calorimetry and spin-lattice relaxation measurements. *Colloid Polym. Sci.* 265, 448–457.
- Eccleston, G.M., 1986. The microstructure of semisolid creams. *Pharm. Int.* 7, 63–70.
- Eccleston, G.M., Behan-Martin, M.K., Jones, G.R., Towns-Andrews, E., 2000. Synchrotron X-ray investigations into the lamellar gel phase formed in pharmaceutical creams prepared with cetrimide and fatty alcohols. *Int. J. Pharm.* 203, 127–139.
- Glatter, Kratky, O., 1982. Small angle X-ray scattering.
- Gstirner, F., Meisenberg, R., 1970. Rheological properties and composition of petrolatum. *Arch. Pharm. Ber. Dtsch. Pharm. Ges.* 303, 872–881.
- Junginger, H., 1984. Colloidal structures of O/W creams. *Pharm. Weekbl.* 6, 141–149.
- Junginger, H.E., 1997. Multiphase emulsions. In: *Surfactants in Cosmetics*, second ed. [M. Dekker]. pp. 155–182.
- Microcrystalline Wax and Petrolatum: Global Market Analysis and Opportunities [WWW Document], n.d. URL: < http://www.klinegroup.com/reports/microcrystalline_wax_petrolatum.asp > (accessed 11.02.17).
- Narayanan, T., Wacklin, H., Konovalov, O., Lund, R., 2017. Recent applications of synchrotron radiation and neutrons in the study of soft matter. *Crystallogr. Rev.* 23, 160–226. <http://dx.doi.org/10.1080/0889311X.2016.1277212>.
- Pajor, Z., Pandula, E., Peres, T., 1967. Elektronenmikroskopische Untersuchung der Salbenstruktur I: Untersuchung von Vaseline. *Fette Seifen Anstrichm.* 69, 855–856. <http://dx.doi.org/10.1002/lipi.19670691108>.
- Pandey, P., Ewing, G.D., 2008. Rheological characterization of petrolatum using a controlled stress rheometer. *Drug Dev. Ind. Pharm.* 34, 157–163. <http://dx.doi.org/10.1080/03639040701484569>.
- Park, E.K., Song, K.W., 2010. Rheological evaluation of petroleum jelly as a base material in ointment and cream formulations: Steady shear flow behavior. *Arch. Pharm. Res.* 33, 141–150. <http://dx.doi.org/10.1007/s12272-010-2236-4>.
- Patterson, A.L., 1939. The scherrer formula for X-ray particle size determination. *Phys. Rev.* 56, 978–982. <http://dx.doi.org/10.1103/PhysRev.56.978>.
- Pena, L.E., Lee, B.L., Stearns, J.F., 1994. Structural rheology of a model ointment. *Pharm. Res.* <http://dx.doi.org/10.1023/A:1018990010686>.
- Pénzes, T., Csóka, I., Erős, I., 2004. Rheological analysis of the structural properties affecting the percutaneous absorption and stability in pharmaceutical organogels. *Rheol. Acta* 43, 457–463. <http://dx.doi.org/10.1007/s00397-004-0396-1>.
- Petersson, M., Gustafson, I., Stading, M., 2008a. Comparison of microstructural and physical properties of two petroleum waxes. *J. Mater. Sci.* 1869–1879. <http://dx.doi.org/10.1007/s10853-007-2417-9>.
- Petersson, M., Gustafson, I., Stading, M., 2008b. Ageing of two petroleum waxes. *J. Mater. Sci.* 43, 1859–1868. <http://dx.doi.org/10.1007/s10853-007-2416-x>.
- van Heugten, A.J.P., Braal, C.L., Versluijs-Helder, M., Vromans, H., 2017a. The influence of cetomacrogol ointment processing on structure: a definitive screening design. *Eur. J. Pharm. Sci.* 99, 279–284. <http://dx.doi.org/10.1016/j.ejps.2016.12.029>.
- van Heugten, A.J.P., Versluijs-Helder, M., Vromans, H., 2017b. Elucidation of the variability in consistency of pharmacopoeia quality petrolatum. *Drug Dev. Ind. Pharm.* 43, 595–599. <http://dx.doi.org/10.1080/03639045.2016.1274902>.
- Yamamoto, Y., Fukami, T., Koide, T., Onuki, Y., Suzuki, T., Metori, K., Katori, N., Hiyama, Y., Tomono, K., 2014. Comparative pharmaceutical evaluation of brand and generic clobetasone butyrate ointments. *Int. J. Pharm.* 463, 62–67. <http://dx.doi.org/10.1016/j.ijpharm.2013.12.054>.